JOURNAL OF PROPULSION AND POWER
Vol. 9, No. 2, March–April 1993

Flame Radiation and Acoustic Intensity Measurements in Acoustically Excited Diffusion Flames

T. Y. Chen,* U. G. Hegde,† B. R. Daniel,‡ and B. T. Zinn§
Georgia Institute of Technology, Atlanta, Georgia 30332

This article describes results of an investigation of the mechanisms responsible for the driving of axial instabilities in solid propellant rocket motors. Specifically, the results of two different experimental methods for measuring the driving of axial acoustic fields by sidewall stabilized diffusion flames are compared. These methods utilize laser Doppler velocimetry (LDV) and CH flame radiation measurements, respectively. The results reveal that the interaction between the acoustic field and the flame produces a space-dependent, oscillatory normal velocity component in the flame region, and oscillatory reaction-and heat-release rates, which depend upon the excited acoustic field. The results suggest that the flame either drives or damps the acoustic fields, depending upon the amplitude and frequency of the excited acoustic wave. In addition, these studies show that the flame driving processes vary within the flame region. The results obtained from the flame radiation measurements are in excellent agreement with those obtained using the velocity measurements.

Nomenclature

A = area of interest in Eq. (1)
D = binary diffusion coefficient
I_q = integral defined in Eq. (2)
i = unit vector in x direction
j = unit vector in y direction
P = acoustic intensity flux across a line y = const
p' = pressure oscillation
p'_{pk} = pressure oscillation amplitude
q' = heat release rate oscillations
Re = real
S_{pq} = cross-spectrum of pressure and heat release rate oscillations
T = period of oscillation
t = time
u' = axial velocity oscillation
$\boldsymbol{u}'$ = velocity oscillation vector
V = volume of interest in Eq. (2)
v' = normal (transverse) velocity oscillation
v_{mean} = mean velocity in the normal direction
v'_{pk} = amplitude of v'
x, y = coordinate axes
x_f = flame width
y_f = flame height
ϕ_{pq} = phase between p' and q'
ϕ_{pv} = phase between p' and v'
ω = frequency of oscillation

Introduction

THIS article describes an investigation of the driving of axial instabilities in solid-propellant rocket motors by gas-phase solid propellant flames. The onset of combustion instabilities in rocket motors depends upon the relative gain (i.e., driving) and loss (i.e., damping) mechanisms within the combustor which add and remove energy from the oscillations, respectively. Control of combustion instabilities in solid propellant rocket motors requires identifying and understanding these mechanisms. Important instability driving mechanisms within the rocket motor include flow related mechanisms such as vortex shedding and the response of the unsteady solid propellant combustion process to the flow oscillations. On the other hand, nozzle damping and viscous dissipation are examples of processes that damp rocket instabilities. This article is specifically concerned with developing an understanding of the gas-phase flame processes in the vicinity of the burning propellant surface that contribute to driving of the axial instabilities.

Solid propellant flames are extremely complex. They generally consist of a pyrolyzing solid propellant that supplies gaseous streams of fuel and oxidizer that burn in a complex myriad of premixed and diffusion flames.[1] It has been argued[1] that premixed flames occur above the oxidizer particles (e.g., ammonium perchlorate) and that the diffusion flames are stabilized above the interfaces between the oxidizer particles and the fuel binder. Since premixed and diffusion flames are expected to respond differently to acoustic excitation, the investigation of the driving of solid-propellant flames has been divided into two parts in this research program. In the first part of this study, the contribution of the premixed gas phase flames were studied theoretically and experimentally.[2–4] The second part of the study, described in this article, investigated the response of diffusion flames to axial acoustic fields.

Ideally, it would have been desirable to use samples of actual solid propellants in the investigation of the time-dependent flowfield in their combustion zones. However, the extremely small dimensions of these zones[5] (of the order of 10–100 μ), the smoky nature of the flames, and the high burning rate of solid propellants makes it difficult to perform such measurements in actual solid propellant flames. Thus, researchers have studied these characteristics of unsteady solid-propellant flames in experiments which simulated important features and/or processes of actual solid propellant flames. For example, Kumar et al.[6] used a porous plate burner with gaseous fuel and oxidizer to study the burning characteristics of nonmetallized composite propellants under both steady and oscillatory flow conditions. Price et al.[7] used ammonium perchlorate (AP)-fuel binder sandwiches to study the combustion zone microstructure in order to clarify the mechanisms

Presented as Paper 90-3929 at the AIAA 13th Aeronautics Conference, Tallahassee, FL, Oct. 22–24, 1990; received Sept. 30, 1991; revision received July 16, 1992; accepted for publication Sept. 3, 1992.

*School of Aerospace Engineering; currently Associate Professor, Department of Aeronautical Engineering, Tamkang University, Taiwan, Republic of China.
†School of Aerospace Engineering; currently Supervisor, Microgravity Science Section, Sverdrup Technology, Inc., Lewis Research Center Group, Brook Park, OH. Senior Member AIAA.
‡Senior Research Engineer, School of Aerospace Engineering.
§Regents' Professor, School of Aerospace Engineering. Fellow AIAA.

that control the burning of composite solid propellants in a rocket motor.

Unsteady diffusion flames have been studied in recent years by several authors. Turns et al.[8] experimentally and analytically studied the detailed structure of pulsed turbulent jet diffusion flames. The study showed that the jet diffusion flame is sensitive to pulsing of the fuel stream and that the flame response is largely frequency-dependent. In addition, this study showed that the pulsing causes a significant increase in the local width of the luminous flame. Lewis et al.[9] experimentally investigated the structure of a flame in an unsteady vortical flow using a laminar coflowing jet flame in which a periodic vortical motion was induced by acoustic excitation of the fuel stream. Their study showed that the flame breaks into a series of axisymmetric flamelets which convect and distort under the influence of buoyancy and the vortical flow. Also, relatively high local strains, produced by the vortical motions, were observed in a region where flame extinction occurs. Although these studies provide considerable insight into the structures of diffusion flames in unsteady environments, the driving characteristics of acoustically excited diffusion flames has not been considered in these studies.

In the present study, the driving of axial acoustic fields by diffusion flames, stabilized on the bottom wall of a long duct, has been investigated experimentally. Although this study uses gaseous diffusion flames to investigate the driving by actual solid-propellant flames, it should be pointed out that the investigated flame configuration possesses certain characteristics similar to those found in solid propellant flames. For example, in both cases, an oscillatory multidimensional flame located near a side boundary is interacting with one-dimensional core flow oscillations. However, contrary to solid propellant flames, the dimensions of the investigated diffusion flames permitted experimental probing of these flames under oscillatory environments. A second consequence of the investigated flame dimensions (1-cm high) was that the flame was essentially outside the acoustic boundary layer. On the other hand, a solid propellant flame inside a rocket motor is usually embedded inside the acoustic boundary layer. It is believed, however, that as was the case with the premixed flame studies,[2-4] the findings of this investigation will improve the understanding of the instability driving mechanisms.

This article describes the driving characteristics of the investigated diffusion flames determined using two different experimental methods. In the first approach, pressure transducers and laser Doppler velocimetry (LDV) were used to determine the acoustic pressure and velocity distributions within the flame. The measured data were then used to determine the spatial dependence of acoustic intensity, which in turn, was used to determine the driving/damping characteristics of the flame. In the second approach, Rayleigh's criterion together with measured CH radiation from the flame and acoustic pressures were used to determine the driving/damping of the flame. Results obtained by these two independent measurement techniques are compared and discussed in this article.

Experimental Setup

A diagram of the experimental setup utilized in this study is shown in Fig. 1. It consists of a 2.5-m long, 3.75 × 7.5 cm^2 rectangular duct with a diffusion-flame burner located on its bottom wall. Two acoustic drivers attached to the duct wall, just upstream of the duct exit plane, are used to excite a standing axial acoustic wave of desired amplitude and frequency inside the duct, which simulates the oscillatory flowfield associated with the rocket motor instability. The location of the flame relative to the excited acoustic field can be changed by axial translation of the "hard" termination at the upstream end of the duct. Three pressure transducers mounted on the wall above the burner are used to determine the dynamic pressure and the flame location with respect to the excited standing wave; i.e., they determine whether the flame is located at a pressure node, a pressure antinode, or in-between. During initial testing it was found that even in the absence of a sound field, the established diffusion flames tips would flicker. The cause of this flicker is uncertain, it could be due to buoyant effects. It was found that a wire mesh placed in the flow above the diffusion flame burner surface inhibited this flicker and was subsequently incorporated in the setup. The placement of the screen (approximately 4-cm above the burner surface) did not interfere with any of the pressure, velocity, and radiation measurements performed.

The experimental setup is mounted on a linear, three-axes, translating system, which can be remotely controlled by a computer. This translating system has a resolution of $\frac{1}{2560}$ cm on the vertical axis and $\frac{1}{80}$ cm in the other two directions, which provides very good spatial resolution for the velocity and radiation measurements conducted in this research.

The developed diffusion flame burner is shown in Fig. 2. It simulates the characteristics of the ideal, sandwich-type, propellant samples whose combustion characteristics were investigated in the past.[7,10] It consists of parallel, alternating, oxidizer, and fuel slots, which were arranged in a 3.5 × 6.6 cm^2 rectangle. High-porosity ceramic matrices were installed in each slot to stabilize the flow. The burner contains three, 1.8-mm-wide fuel slots that are much smaller than the 20-mm-wide oxidizer slots, and it produces three small, laminar, overventilated diffusion flames. The oxidizer was injected at the bottom of the burner and part of the oxidizer flow was diverted through a particle seeder (see Fig. 1) with a control valve which allows adjustment of the seeding rate. The seeded oxidizer was injected through a 0.625-cm-diam copper tube with 23 injection holes of 0.8-mm diam to allow LDV measurements. Fuel was injected through the sides of the burner and the central fuel line was seeded with particles (0.2 μ size titanium dioxide) when the LDV measurements were performed. These particles were introduced into the central fuel line by the arrangement shown in Fig. 2, which prevented a

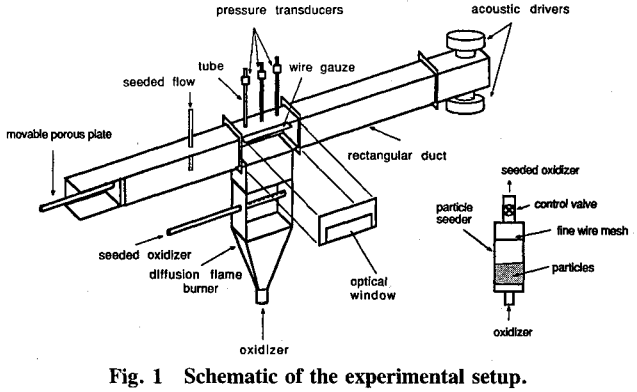

Fig. 1 Schematic of the experimental setup.

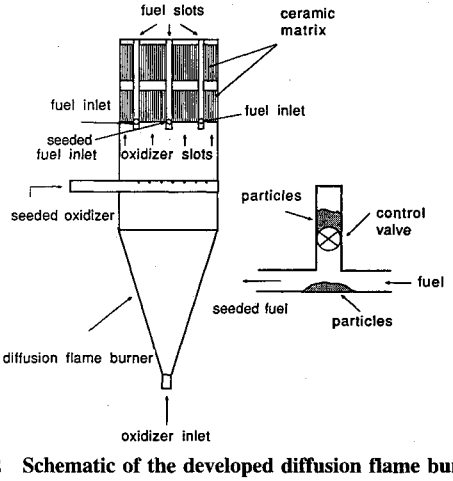

Fig. 2 Schematic of the developed diffusion flame burner.

large pressure drop that would have caused a pressure imbalance between the three fuel supply lines. The oxidizer and fuel flow rates were controlled by separate flow meters. The oxidizer consisted of 31% oxygen, 51% carbon dioxide, and 18% nitrogen by volume. Commercial grade methane, diluted with 49% nitrogen, was used as fuel. These specific compositions produced a blue, soot-free flame which enabled Rayleigh scattering temperature measurements that were also performed within these flames.[11]

The oxidizer and fuel-flow injection velocities were identical at 9 cm/s. The Reynolds number, based upon oxidizer injection conditions, was 130. These low Reynolds numbers ensured laminar injection of fuel and oxidizer. All experiments were conducted at prevailing laboratory conditions which were nominally 1-atmosphere pressure and 25°C. The established flames were approximately 1-cm high and 0.6-cm wide (visible flame). The temperature at the flame sheet was approximately 1900 K and dropped off to around 400 K at the centerlines of the oxidizer slots.[13]

In order to determine the distribution of the acoustic intensity along a direction normal to the burner, the distribution of the component of the acoustic velocity along this normal direction was measured. A single-component, dual-beam, forward-scatter LDV system, with a 5-W argon-ion laser, was utilized. The Doppler signals, detected by a photomultiplier, were processed by a counter-type signal processor. The resulting digital output of the signal processor was transmitted to, and subsequently analyzed, by a minicomputer. In order to measure the amplitude of the oscillatory normal velocity component and the phase difference between the pressure and velocity oscillations, which are important parameters of the acoustic wave-flame interaction, the LDV data were analyzed using a "conditional sampling" technique. This technique permits determination of the periodic velocity behavior by synchronizing the beginning of the sampling interval of the LDV data with respect to the periodic pressure oscillations. This method is similar to that of Bell et al.[12] and Lepicovsky.[13] No special calibration of the LDV is needed; however, note that injection velocities of the oxidizer as measured with the LDV agreed with those calculated from the flow-meter readings.

Radiation from the oscillating flame was collected by a camera lens. A paper shield containing a 0.8-mm-wide and 1.2-cm-long (that is, twice the width of the visible flame) slot was placed, with its long side normal to the flame axis, at desired locations in front of the optical window of the test section in order to permit radiation measurements from specific flame regions. A photomultiplier with optical filter (431 nm for CH) was used to receive the photo current from the flame. This signal was subsequently converted to a measurable voltage. Since, in general, the radiation signal was very weak, a dc amplifier was used to amplify the signal. Dynamic pressures were measured by pressure transducers with dual mode amplifiers. The pressure transducers were mounted on long "semi-infinite" tubes at some distance away from the test section (see Fig. 1) to prevent heat damage, and to provide an adaptor which possessed a flat frequency response. Both the radiation and pressure signals were filtered electronically. The whole system was calibrated to correct for the phase shifts introduced by the filter, amplifier and semi-infinite tubes. In addition, amplitude readings of the pressure transducers were calibrated against known sound source amplitudes. It should be noted that the experiments described in this article were all conducted with the diffusion flame burner located at a pressure maximum of the acoustic wave of interest. This location was obtained by moving the "hard" termination at the upstream end of the duct and monitoring the pressure transducers readings. When a pressure maximum was reached, the transducers output would be the highest; note also that the readings of the three transducers under these conditions were almost identical for the frequencies considered, indicating that the pressure in the burner region was spatially invariant.

Software was developed for performing on-line digital data acquisition and time-series analysis of the digitized data using an FFT algorithm. The phase difference between the radiation and pressure oscillations were obtained from the cross spectrum of their signals, whereas, the amplitudes of the radiation and pressure signals were determined from their individual autospectrum.

Results and Discussions

In the first approach, the driving characteristics of the flame were determined from measured variations of the acoustic power generated (or absorbed) in a given area of the flame. This involves evaluation of the distribution of the integral

$$\int_A \int_T \boldsymbol{I}\cdot\boldsymbol{n}\ \mathrm{d}t\ \mathrm{d}A = \int_A \int_T p'\boldsymbol{u}'\cdot\boldsymbol{n}\ \mathrm{d}t\ \mathrm{d}A \qquad (1)$$

where $\boldsymbol{I}, A, T, p', \boldsymbol{u}'\ (=u'\boldsymbol{i} + v'\boldsymbol{j})$ and $\boldsymbol{n}$ are the local acoustic intensity flux, the relevant area of interest, the period of the oscillation, the pressure oscillation, the velocity oscillation vector, and the local outward normal to the area A, respectively. This integral determines whether a net amount of energy is generated or absorbed within the investigated region which corresponds to "driving" and "damping" by this region, respectively. Thus, when the integral is positive, a net amount of acoustic energy leaves the region A, implying that acoustic energy is generated within A.

The present study investigated the response of the flames to acoustic excitation when they were located at a pressure antinode which corresponds to a node of the axial velocity oscillations u'; i.e., u' may be set to zero. It is then appropriate to modify Eq. (1) to obtain the variations in acoustic power (or intensity) as a function of the normal distance from the burner surface. Thus, at any location y (see Fig. 3), the factor $\boldsymbol{u}'\cdot\boldsymbol{n}\ \mathrm{d}A$ in Eq. (1) is replaced by the product $v'\ \mathrm{d}x$. Furthermore, p' is assumed to be spatially invariant over the flame region since the flame response was studied at frequencies having acoustic wavelengths much longer than the dimensions of the flame (e.g., 2 cm). In addition, without loss of generality, all phase angles were referred to the pressure in the flame region which, therefore, may be taken to be a real quantity. Consequently, the expression for the acoustic flux P across the line y = const is given by

$$P(y) = 0.5p'_{pk}\int_L \mathrm{Re}(v')\ \mathrm{d}x$$

where p'_{pk} is the amplitude of the pressure oscillation and L is the length of interest in the x direction which, here, is the distance between the centerlines of the two oxidizer slots on each side of the flame (see Fig. 3). Note also that

$$\mathrm{Re}(v') = v'_{pk}\cos\phi_{pv}$$

where ϕ_{pv} is the phase between p' and v', and v'_{pk} is the amplitude of v'.

Thus, the driving in a flame region (see Fig. 3) bounded, e.g., by the horizontal lines $y = y_1$ and $y = y_2$ may be determined by evaluating the acoustic intensity integrals (denoted by P_1 and P_2) along these lines. This region drives the waves when $\Delta P = P_2 - P_1$ is positive and vice versa. Consequently, the considered flame region drives the oscillations when

$$\left[\int_L \mathrm{Re}(v')\ \mathrm{d}x\right]_{y=y2} > \left[\int_L \mathrm{Re}(v')\ \mathrm{d}x\right]_{y=y1}$$

The above expression implies that if $\int \mathrm{Re}(v')\ \mathrm{d}x$ increases with y in a given flame region, then the flame tends to drive

the acoustic oscillations in this region, and vice versa. Consequently, by measuring the distribution of the normal velocity amplitude v'_{pk}, and the phase relationship ϕ_{pv}, between the pressure and velocity oscillations in the flame region, the driving/damping characteristics of the investigated diffusion flames can be determined.

A typical, measured time dependence of the normal velocity component at a point in the flame region near the flame tip exposed to a 400-Hz acoustic field is shown in Fig. 4. This figure indicates that the axial acoustic field produces an oscillatory, normal flow velocity component having the same frequency as the imposed acoustic oscillations. The amplitude of the oscillatory velocity v'_{pk}, and the phase relationship ϕ_{pv}, between pressure and velocity oscillations can be obtained from this figure by "fitting" (using the method of least-square approximation) the measured velocity variation with a function of the form

$$v_{\text{fit}} = v_{\text{mean}} + v'_{pk} \cos(\omega t + \phi_{pv})$$

where v_{mean} is the mean of the measured velocity. Having determined v'_{pk} and ϕ_{pv}, the real part of the oscillatory normal velocity, Re(v'), can be computed at locations of interest and used to determine the driving/damping characteristics of the investigated flames.

Figure 5 shows the x dependence of Re(v') measured at two different amplitudes (110 and 120 dB) of a 300-Hz acoustic field. This figure shows that a higher excitation amplitude produces a larger magnitude of Re(v'). It is also noted that the magnitude of Re(v') reaches a maximum in the vicinity of the flame sheet location. The dependence of the x distribution of Re(v') upon the frequency of acoustic waves was also investigated. Figure 6 describes this dependence for two different driving frequencies (300 and 400 Hz), and it shows that the magnitude of Re(v') is frequency-dependent. The pressure amplitude in both cases was 120 dB.

In this study, the driving/damping characteristics of the flame were investigated by evaluating $\int$ Re(v') dx at different y locations. Figures 7 and 8 present the y dependence of $\int$ Re(v') dx (normalized with its absolute value at $y = 0$) measured at two different driving frequencies with the flame located at a pressure antinode. The integrand was calculated at 55 equally spaced x positions between the centerlines of the two oxidizer slots adjoining the central fuel slot (i.e., between $x = -1$ and $x = 1$ in Fig. 3) for each y location. Figure 7 shows that for a 300-Hz excitation $\int$ Re(v') dx in-

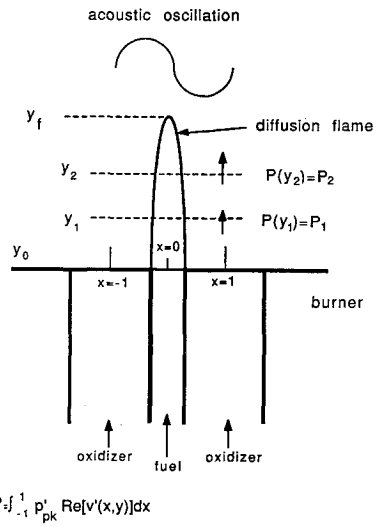

Fig. 3 Determination of flame driving from v' and p' measurements. Driving occurs in a given region $\Delta y = y_2 - y_1$ bounded by $x = -1$ and $x = 1$ when $\Delta P = P_2 - P_1 > 0$.

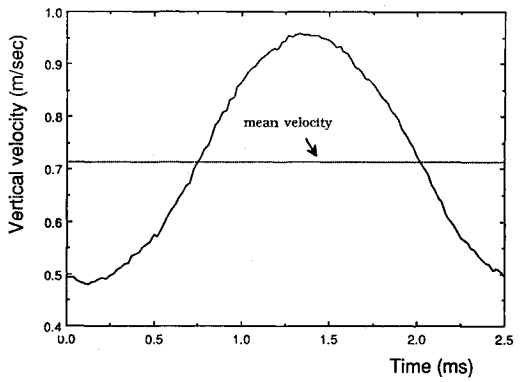

Fig. 4 Typical time trace of the normal velocity at a pressure antinode of a 400-Hz oscillation.

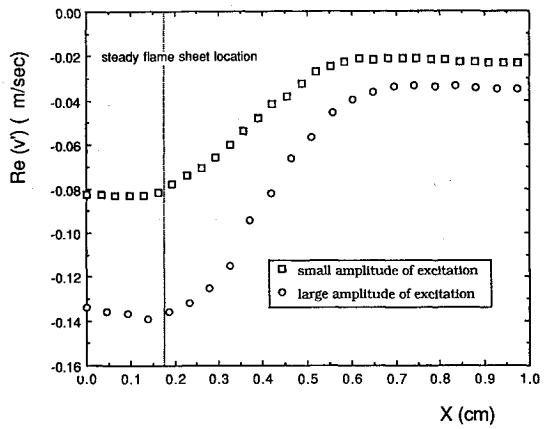

Fig. 5 Comparison of measured Re(v') distributions at $y = y_f$ with large (120 dB) and small (110 dB) acoustic excitations.

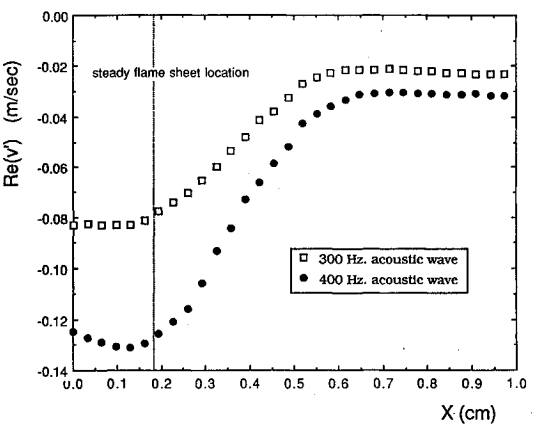

Fig. 6 Comparison of measured Re(v') distributions at $y = y_f$ for two different excitation frequencies.

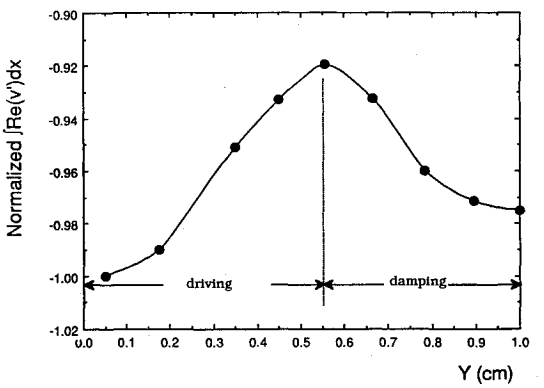

Fig. 7 Measured spatial dependence of $\int$ Re(v') dx as a function of y for 300-Hz excitation.

creases continually up to $y = 0.55y_f$ (where y_f is the flame height) and that it subsequently decreases. Based upon the above discussion, this result indicates that when the flame is subjected to a 300-Hz acoustic oscillation, the lower [where $\int \mathrm{Re}(v')\,dx$ increases] and upper [(where $\int \mathrm{Re}(v')\,dx$ decreases] regions of the flame drive and damp the oscillation, respectively. The overall driving/damping of the flame depends upon the net effect of these two regions. Since, $[\int \mathrm{Re}(v')\,dx]_{y=y_f} > [\int \mathrm{Re}(v')\,dx]_{y=0}$, the net effect of the flame, in this case is to drive the acoustic field. Figure 8 shows that $\int \mathrm{Re}(v')\,dx$ increases continually along the whole length of the flame when the flame interacts with a 400-Hz acoustic field, indicating that driving occurs throughout the flame region. In summary, the measured oscillatory velocity data indicate that the investigated diffusion flames both drive and damp the acoustic waves, and that the magnitudes of these processes vary within the flame region. In addition, this study shows that the driving/damping characteristics of the investigated flames are frequency dependent.

It should be noted that the original LDV setup could not measure the normal velocity near $y = 0$, because one of the laser beams was blocked by the burner wall. To overcome this problem, the whole experimental setup was rotated by approximately 6 deg toward the LDV system. The velocity measured in such a configuration could not be the same as the normal velocity measured when the setup was not rotated. However, if the flowfield is rotated out of vertical by an angle less than 6 deg, the error introduced is less than 0.5%,[11] which is acceptable.

Flame radiation measurements are of interest because earlier studies[3,14] have shown that the radiation intensities from radicals such as CH, CC, and OH are proportional to the reaction and heat release rates in the flame. Such radiation measurements were used in this study to determine the effects of the acoustic field upon the reaction- and heat-release rates, and the phase relationship between the heat release and pressure oscillations. The latter is important because, as stated by Rayleigh's criterion,[15] the phase relationship determines whether the flame adds or removes energy from the acoustic waves. Expressed mathematically,[16] an oscillatory heat source (such as a flame) adds energy to the acoustic waves when the following inequality is satisfied:

$$I_q = \int_v |S_{pq}| \cos \phi_{pq}\, dV > 0 \qquad (2)$$

where $|S_{pq}|$ and ϕ_{pq} are the magnitude of the cross spectrum between p' and q' oscillations, and the phase difference between p' and q', respectively. The above integration is performed over the whole space, V, where driving or damping by the flame occurs. In a flame region where the integrand is positive, driving of the acoustic waves occurs. This integrand is positive where p' and q' are in phase; that is, where -90 deg $< \phi_{pq} <$ 90 deg. On the other hand, damping of the acoustic field by the flame occurs when p' and q' are out of phase.

In the present study, CH flame radiation measurements were carried out at different wave frequencies and different regions of the flame. These studies revealed that the autospectrum of the overall flame radiation exhibits a peak at the same frequency as the measured pressure autospectrum, and that the amplitude of the peak is proportional to the amplitude of the pressure oscillation (110 and 120 dB), see Figs. 9 and 10. These results indicate that the presence of an acoustic field results in periodic reaction and heat release rates having the same frequency as the imposed acoustic field. Also, the magnitude of the periodic heat release process is proportional to the amplitude of the acoustic waves, which suggests that a higher amplitude of acoustic excitation would result in a higher driving/damping effect.

The magnitudes of the flame radiation and the phase differences between the pressure and radiation oscillations at

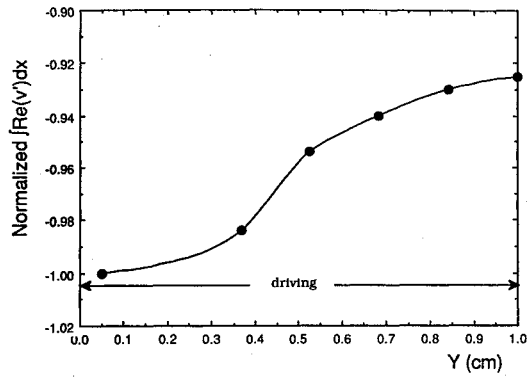

Fig. 8 Measured spatial dependence of $\int \mathrm{Re}(v')\,dx$ as a function of y for 400-Hz excitation.

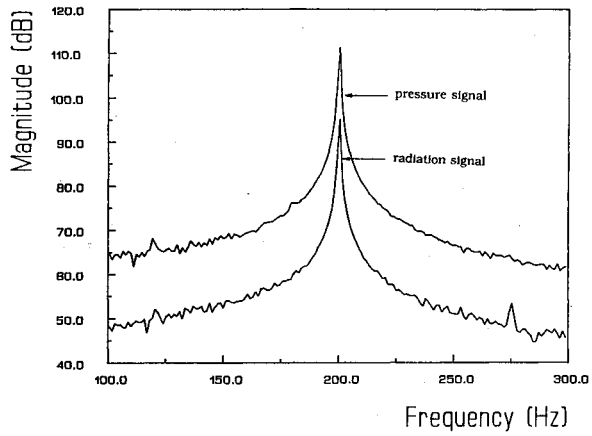

Fig. 9 Autospectra of pressure and radiation oscillations for 200-Hz excitation.

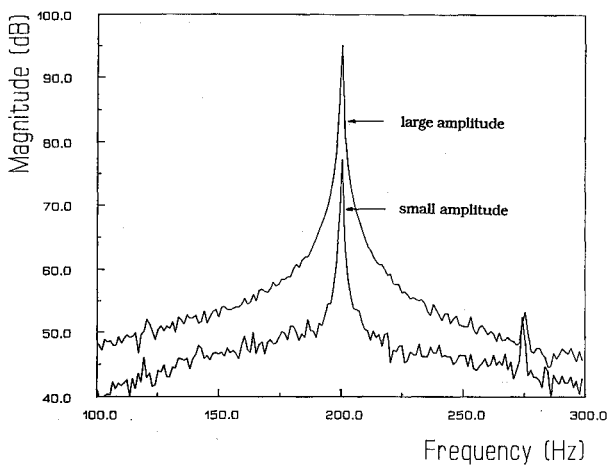

Fig. 10 Autospectra of radiation oscillations with large (120 dB) and small (110 dB) acoustic excitations.

different sections of the flame region were also investigated. These data were then used to determine the driving/damping behavior at different flame regions. Specifically, the variation of the flame driving along a line normal to the burner surface was studied. Figure 11 describes the response of the flame to a 300-Hz acoustic wave. This figure shows that the measured magnitude of flame radiation signal and the phase difference between pressure and radiation oscillations were space-dependent. In addition, they exhibited a "jump" between the lower and upper parts of the flame. The cause of this jump is presently unclear; however, it was also observed when the flame was exposed to a 400-Hz acoustic excitation, as shown in Fig. 12. In both cases, the measured phase data show that the jump in phase is approximately 170 deg. However, different driving and damping effects within the flame region

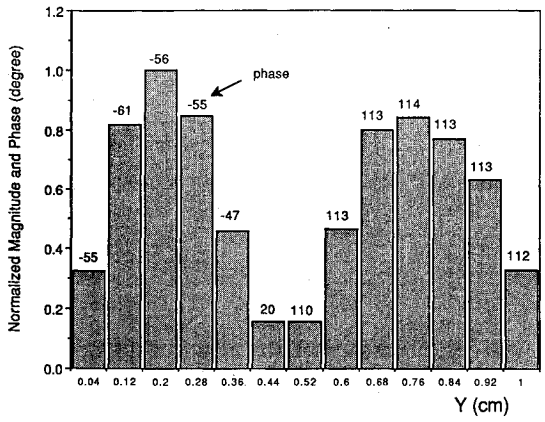

Fig. 11 Measured magnitude and phase of radiation oscillations as functions of y for 300-Hz acoustic excitation.

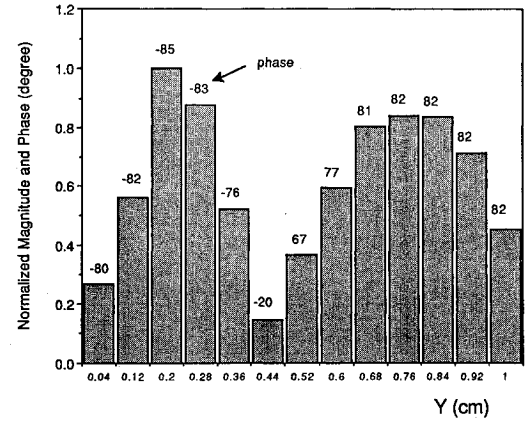

Fig. 12 Measured magnitude and phase of radiation oscillations as functions of y for 400-Hz acoustic excitation.

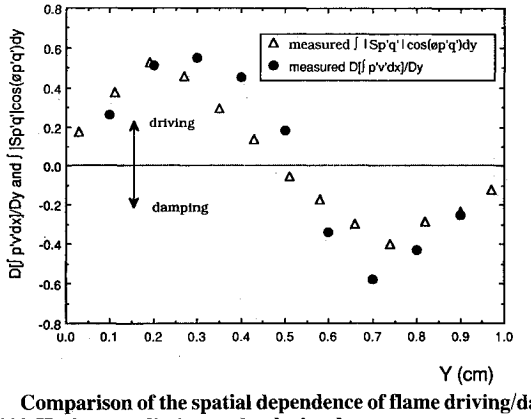

Fig. 13 Comparison of the spatial dependence of flame driving/damping at 300 Hz from radiation and velocity data.

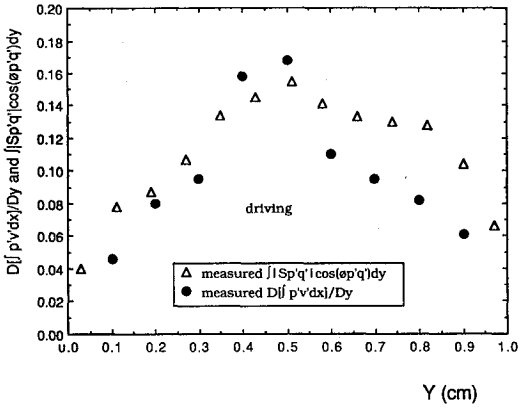

Fig. 14 Comparison of the spatial dependence of flame driving/damping at 400 Hz from radiation and velocity data.

were observed. For the 300-Hz acoustic wave, driving (i.e., $\phi_{pq} < 90$ deg) occurs in the lower part of the flame, while damping (i.e., $\phi_{pq} > 90$ deg) occurs in its upper part. On the other hand, for the 400-Hz wave, the measured phase differences between the pressure and radiation oscillations show that the flame drives (i.e., $\phi_{pq} < 90$ deg) the acoustic wave along the entire length of the flame.

By choosing V in Eq. (2) to be the volume of the flame that the radiation slot "sees" at any given y location of the slot, the integral I_q [see Eq. (2)] can be evaluated at different heights above the burner surface. This variation of I_q describes the flame driving/damping as a function of y. These results were also compared with those obtained from the LDV measurements, see Figs. 13 and 14. In these two figures, $D[\int \mathrm{Re}(v')\,dx]/Dy$ describes the difference between the normalized [with respect to the value of $\int \mathrm{Re}(v')\,dx$ at $y = 0$] acoustic energy fluxes entering and leaving a horizontal slice of the flame parallel to the x axis and having a thickness Δy ($=0.1y_f$; note $y_f = 1$ cm). Driving occurs in this slice when $D[\int \mathrm{Re}(v')\,dx]/Dy > 0$, and damping occurs when $D[\int \mathrm{Re}(v')\,dx]/Dy < 0$. These figures show that the findings of the flame radiation and oscillatory velocity studies are in excellent agreement. Both measurements show that in the case of a 300-Hz acoustic wave, the flame region near the burner (i.e., $0 < y < 0.55y_f$) drives the wave and the remainder of the flame damps the wave. For the case of the 400-Hz acoustic field, both measurements show that the flame drives the acoustic wave throughout the whole flame region and, thus, the overall effect of the flame is to drive the acoustic wave. In addition, these results show that the driving and damping are very small in the middle section of the flame for a 300-Hz wave, while the driving reaches a maximum in the middle section of the flame for a 400-Hz wave.

At this stage, the apparently frequency-dependent mechanisms which cause the different driving and damping characteristics within the two diffusion flames are not fully understood. However, measurements, utilizing the classical impedance tube technique,[17] show that there are significant differences between the burner admittance, R_v [$=(v'/p')_{y=0}$] at 300 and 400 Hz. Figure 15 plots the measured values of the real and imaginary parts of the burner admittance as a function of frequency. The admittance values have been normalized utilizing the values of mean injection velocity and pressure. It is possible that this frequency dependence of the admittance contributes to the observed variation in flame driving/damping behavior at the two frequencies.

Frequency-dependent combustion processes may also contribute to the observed differences. The diffusion velocity of the reactants toward the flame is estimated to be of the order of $2D/x_f$ where D is a representative diffusion coefficient. The value of D for methane at representative flame temperatures

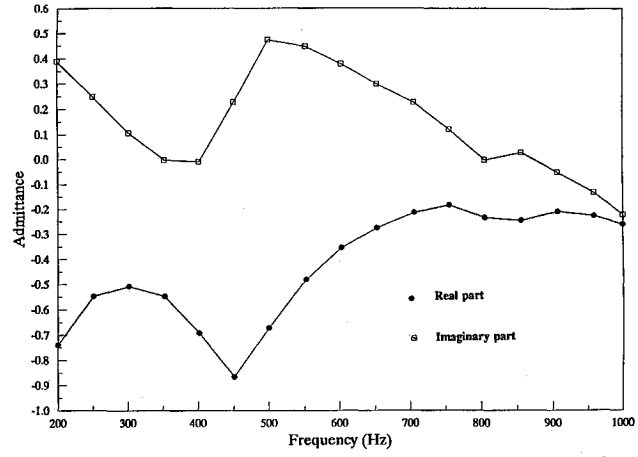

Fig. 15 Frequency dependence of the real and imaginary parts of the burner surface acoustic admittance.

is 1 cm^2/s which yields diffusion velocities of the order of 4 cm/s. This is of the same order as the acoustic velocities (10 cm/s, see Figs. 5 and 6). This indicates that the acoustic field has an important influence on the arrival of reactants, and their subsequent combustion, at the flame front. It is satisfactory to note, however, that the results obtained using two independent (i.e., flame radiation and velocity) measurements are in excellent agreement.

Conclusions

Velocity and flame radiation measurements conducted under this study show that the interaction between diffusion flames and axial acoustic fields produces an oscillatory normal velocity component within the flames and oscillatory reaction and heat release rates. The characteristics of this oscillatory behavior depend upon the location within the flame region, the frequency and the amplitude of the acoustic wave. The measurements show that the magnitudes of the oscillatory velocity and the flame radiation increase as the amplitude of the acoustic wave increases, indicating that the driving/damping of the flame is proportional to the amplitude of the excited wave. Furthermore, both measurements reveal that the driving/damping characteristics of the investigated diffusion flames strongly depend upon the frequency of the acoustic excitation and that the flame driving/damping varies along the flame. Finally, the results obtained from the independent velocity and flame radiation measurements are in excellent agreement.

Acknowledgment

This work was supported by the Air Force Office of Scientific Research under Grant AFOSR-84-0082; Mitat A. Birkan, Grant Monitor.

References

[1]Beckstead, M. W., Derr, R. L., and Price, C. F., "A Model of Composite Solid Propellant Based on Multiple Flames," *AIAA Journal*, Vol. 8, No. 12, 1970, pp. 2200–2207.

[2]Hegde, U. G., and Zinn, B. T., "The Acoustic Boundary Layer in Porous Walled Ducts with a Reacting Flow," *Proceedings of the Twenty-First Symposium (International) on Combustion*, Combustion Inst., Pittsburgh, PA, Aug. 1986, pp. 1993–2000.

[3]Sankar, S. V., Hegde, U. G., Jagoda, J. I., and Zinn, B. T., "Driving of Axial Acoustic Waves by Side Wall Stabilized Premixed Flames," *Proceedings of the Twenty-Second Symposium (International) on Combustion*, Combustion Inst., Pittsburgh, PA, Aug. 1988, pp. 1371–1380.

[4]Sankar, S. V., Jagoda, J. I., Daniel, B. R., and Zinn, B. T., "Measured and Predicted Characteristics of Premixed Flames Stabilized in Axial Acoustic Fields," AIAA Paper 88-0541, Jan. 1988.

[5]"Fundamentals of Solid-Propellant Combustion," edited by K. K. Kuo, and M. Summerfield, Progress in Astronautics and Aeronautics, Vol. 90, AIAA, New York, 1984.

[6]Kumar, R. N., Strand, L. D., and McNamara, R. P., "Composite Propellant Combustion Modelling with a Porous Plate Burner," AIAA Paper 76-669, 1976.

[7]Price, E. W., Sambamurthi, R. K., Sigman, R. K., and Panyam, R. R., "Combustion of Ammonium Perchlorate-Polymer Sandwiches," *Combustion and Flame*, Vol. 63, No. 3, 1986, pp. 381–413.

[8]Turns, S. R., Merkle, C. L., Lovett, J. A., and Hosangadi, A., "Mixing and Combustion of Pulsed Gas Jets," Annual Rept. to Gas Research Inst., Pennsylvania State Univ., University Park, PA, 1988.

[9]Lewis, G. S., Cantwell, B. J., Vandsburger, U., and Bowman, C. T., "An Investigation of the Structure of a Laminar Non-Premixed Flame in an Unsteady Vortical Flow," *Proceedings of the Twenty-Second Symposium (International) on Combustion*, Combustion Inst., Pittsburgh, PA, Aug. 1988, pp. 515–522.

[10]Brown, W. E., Kennedy, J. R., and Zetzer, D. W., "An Experimental Study of Ammonium Perchlorate-Binder Sandwich Combustion in Standard and High Acceleration Environments," *Combustion Science and Technology*, Vol. 6, No. 4, 1972, pp. 211–222.

[11]Chen, T., Ph.D. Dissertation, Georgia Inst. of Technology, Atlanta, GA, 1990.

[12]Bell, W. A., and Lepicovsky, J., "Conditional Sampling with a Laser Velocimeter," AIAA Paper 83-0756, 1983.

[13]Lepicovsky, J., "Laser Velocimeter Measurements of Large Scale Structures in a Tone-Excited Jet," *AIAA Journal*, Vol. 24, No. 1, 1986, pp. 27–31.

[14]Hurle, I. R., Price, R. B., Sugden, T. M., and Thomas, A., "Sound Emission from Open Turbulent Premixed Flames," *Proceedings of the Royal Society of London; Mathematical and Physical Sciences*, Vol. 303, No. 1475, 1968, pp. 409–428.

[15]Lord Rayleigh, *The Theory of Sound*, Vol. II, Dover, New York, 1945, pp. 224–235.

[16]Putnam, A. A., *Non-Steady Flame Propagation*, edited by G. H. Markstein, Pergamon, New York, 1964, Chap. F, pp. 183–198.

[17]Pierce, A. D., *Acoustics: An Introduction to its Principle and Application*, McGraw-Hill, New York, 1981.